

Superoutburst of SDSS J090221.35+381941.9: First Measurement of Mass Ratio in an AM CVn-Type Object using Growing Superhumps

Taichi KATO,^{1*} Tomohito OHSHIMA,¹ Denis DENISENKO,² Pavol A. DUBOVSKY,³ Igor KUDZEJ,³ William STEIN,⁴ Enrique de MIGUEL,^{5,6} Arne HENDEN,⁷ Ian MILLER,⁸ Kirill ANTONYUK,⁹ Oksana ANTONYUK,⁹ Nikolaž PIT,⁹ Aleksei SOSNOVSKIJ,⁹ Alex BAKLANOV,⁹ Julia BABINA,⁹ Elena P. PAVLENKO,^{9,1} Kazunari MATSUMOTO,¹⁰ Daiki FUKUSHIMA,¹⁰ Megumi TAKENAKA,¹⁰ Miho KAWABATA,¹⁰ Daisuke DAISUKE,¹⁰ Kazuki MAEDA,¹⁰ Risa MATSUDA,¹⁰ Katsura MATSUMOTO,¹⁰ Colin LITTLEFIELD,¹¹ Arto OKSANEN,¹² Hiroshi ITOH,¹³ Gianluca MASI,¹⁴ Francesca NOCENTINI,¹⁴ Patrick SCHMEER,¹⁵ Roger D. PICKARD,^{16,17} Seiichiro KIYOTA,¹⁸ Shawn DVORAK,¹⁹ Joseph ULOWETZ,²⁰ Yutaka MAEDA,²¹ Raúl MICHEL,²² Sergey Yu. SHUGAROV,^{23,24} Drahomir CHOCHOL,²⁴ Rudolf NOVÁK,²⁵

¹ Department of Astronomy, Kyoto University, Kyoto 606-8502

*tkato@kusastro.kyoto-u.ac.jp

² Space Research Institute (IKI), Russian Academy of Sciences, Moscow, Russia

³ Vihorlat Observatory, Mierova 4, Humenne, Slovakia

⁴ 6025 Calle Paraiso, Las Cruces, New Mexico 88012, USA

⁵ Departamento de Física Aplicada, Facultad de Ciencias Experimentales, Universidad de Huelva, 21071 Huelva, Spain

⁶ Center for Backyard Astrophysics, Observatorio del CIECEM, Parque Dumar, Matalascañas, 21760 Almonte, Huelva, Spain

⁷ American Association of Variable Star Observers, 49 Bay State Rd., Cambridge, MA 02138, USA

⁸ Furzehill House, Ilston, Swansea, SA2 7LE, UK

⁹ Crimean Astrophysical Observatory, Kyiv Shevchenko National University, 98409, Nauchny, Crimea, Ukraine

¹⁰ Osaka Kyoiku University, 4-698-1 Asahigaoka, Osaka 582-8582

¹¹ Department of Physics, University of Notre Dame, Notre Dame, Indiana 46556, USA

¹² Hankasalmi observatory, Jyvaskylan Sirius ry, Vertaalantie 419, FI-40270 Palokka, Finland

¹³ Variable Star Observers League in Japan (VSOLJ), 1001-105 Nishiterakata, Hachioji, Tokyo 192-0153

¹⁴ The Virtual Telescope Project, Via Madonna del Loco 47, 03023 Ceccano (FR), Italy

¹⁵ Bischmisheim, Am Probstbaum 10, 66132 Saarbrücken, Germany

¹⁶ The British Astronomical Association, Variable Star Section (BAA VSS), Burlington House, Piccadilly, London, W1J 0DU, UK

¹⁷ 3 The Birches, Shobdon, Leominster, Herefordshire, HR6 9NG, UK

¹⁸ VSOLJ, 7-1 Kitahatsutomi, Kamagaya, Chiba 273-0126

¹⁹ Rolling Hills Observatory, 1643 Nightfall Drive, Clermont, Florida 34711, USA

²⁰ Center for Backyard Astrophysics Illinois, Northbrook Meadow Observatory, 855 Fair Ln, Northbrook, Illinois 60062, USA

²¹ Kaminishiyamamachi 12-14, Nagasaki, Nagasaki 850-0006

²² Instituto de Astronomía UNAM, Apartado Postal 877, 22800 Ensenada B.C., México

²³ Sternberg Astronomical Institute, Lomonosov Moscow University, Universitetsky Ave., 13, Moscow 119992, Russia

²⁴ Astronomical Institute of the Slovak Academy of Sciences, 05960, Tatranska Lomnica, the Slovak Republic

²⁵ Research Centre for Toxic Compounds in the Environment, Faculty of Science, Masaryk University, Kamenice 3, 625 00 Brno, Czech Republic

(Received 201 0; accepted 201 0)

Abstract

We report on a superoutburst of the AM CVn-type object SDSS J090221.35+381941.9 [J0902; orbital period 0.03355(6) d] in 2014 March–April. The entire outburst consisted of a precursor outburst and the main superoutburst, followed by a short rebrightening. During the rising branch of the main superoutburst, we detected growing superhumps (stage A superhumps) with a period of 0.03409(1) d. During the plateau phase of the superoutburst, superhumps with a shorter period (stage B superhumps) were observed. Using the orbital period and the period of the stage A superhumps, we were able to measure the dynamical precession rate of the accretion disk at the 3:1 resonance, and obtained a mass ratio (q) of 0.041(7). This is the first successful measurement of the mass ratio in an AM CVn-type object using the recently developed stage A superhump method. The value is generally in good agreement with the theoretical evolutionary model. The orbital period of J0902 is the longest among the outbursting AM CVn-type objects, and the borderline between the outbursting systems and systems with stable cool disks appears to be longer than had been supposed.

Key words: accretion, accretion disks — stars: novae, cataclysmic variables — stars: dwarf novae —

stars: individual (SDSS J090221.35+381941.9)

1. Introduction

AM CVn-type objects are a class of cataclysmic variables (CVs) composed of an accreting white dwarf and a mass-transferring helium white dwarf (secondary star). The orbital periods (P_{orb}) of AM CVn-type objects are in a range of 5 and 65 min, and comprise the population of the shortest- P_{orb} CVs [for recent reviews of AM CVn-type objects, see e.g. Nelemans (2005); Solheim (2010)].

AM CVn-type objects have recently been becoming an interesting topic in astrophysics because some of them are considered as the most promising objects for direct detection of the gravitational wave radiation (e.g. Nelemans 2003). Some AM CVn-type objects are also considered as progenitors of a population of type-Ia supernovae (Solheim, Yungelson 2005). Three evolutionary paths have been proposed to form AM CVn-type objects, and they have been widely discussed both in terms of theoretical population synthesis and observations (see e.g. Solheim 2010).

Still, basic parameters of AM CVn-type objects, such as mass ratios ($q = M_2/M_1$), are difficult to measure observationally and this difficulty has hindered the comparison between the theory and observation. This difficulty partly comes from the difficulty in directly detecting the secondary and there have been attempts to estimate the mass ratios by using the Doppler tomography of the accretion disk (Marsh 1999; Nelemans et al. 2001b; Roelofs et al. 2006).

Many AM CVn-type objects show superhumps, which arise as a result of the precession of the eccentric accretion disk deformed by the 3:1 resonance with the secondary (Whitehurst 1988; Hirose, Osaki 1990). The fractional superhump excess ($\varepsilon \equiv P_{\text{SH}}/P_{\text{orb}} - 1$, where P_{SH} is the superhump period) reflects the precession rate, and the empirical relation between ε and q (such as Patterson 1998, Patterson et al. 2005), which has been developed and calibrated for hydrogen-rich CVs, has been used to estimate the q values.

This method, however, suffers from the unknown degree of the pressure effect (e.g. Pearson 2007). There has been only one direct measurement of the q value in an AM CVn-type object by analyzing eclipses in SDSS J092620.42+034542.3 (Copperwheat et al. 2011). The only other known eclipsing AM CVn-type object, PTF1 J191905.19+481506.2, is only partially eclipsing and the q value has not been determined (Levitan et al. 2014).

In the last two years, however, there has been a great progress in understanding the precession rate in the superhumping accretion disk, and it has become clear that the superhumps in the growing stage during the superoutburst reflects the dynamical precession rate at the radius of the 3:1 resonance (Kato, Osaki 2013). Although this method was initially developed for hydrogen-rich CVs, it is expected to be applicable to AM CVn-type objects since it only depends on dynamics. Here, we present the first

successful result.

2. SDSS J090221.35+381941.9

SDSS J090221.35+381941.9 (hereafter J0902) is an AM CVn-type object selected by color using the Sloan Digital Sky Survey (SDSS) (Rau et al. 2010). Rau et al. (2010) obtained time-resolved spectra of this object and identified the orbital period of 48.31(8) min [0.03355(6) d] from the radial velocity variations of the emission lines. Although the continuum could be well reproduced by a blackbody of 15000 K, the lack of the broad absorption lines suggested that the accreting white dwarf is either cooler than 15000 K or the additional component contributes to the continuum.

The emission-line spectrum in Rau et al. (2010) was indicative of an AM CVn-type object with a cold, quiescent disk, unlike a thermally stable disk as in AM CVn. No outburst was recorded in this system in the past.

On 2014 March 6, D. Denisenko detected an outburst from the MASTER-Kislovodsk (see Gorbovskoy et al. 2013 for the MASTER network) images (vsnet-alert 16982).¹ The object experienced a very rapid fading (vsnet-alert 16986, 16988) at a rate of 2.3–2.9 mag d⁻¹. This outburst turned out to be a precursor outburst. The object started rising on March 12 (vsnet-alert 17016) and went into a superoutburst on March 15–16 accompanied by developing superhumps (vsnet-alert 17023).

3. Observation and Analysis

The data were acquired by time-resolved unfiltered and V-band CCD photometry using 30–40cm class telescopes by the VSNET Collaboration (Kato et al. 2004) and the public data from the AAVSO International Database.² All the observed times were corrected to Barycentric Julian Date (BJD). Before making the analysis, we corrected zero-point differences between different observers by adding a constant to each observer. For the outbursting CVs, the magnitude system of the unfiltered CCD observations is close to V . The details of the observations will be presented in a separate paper.

The data analysis was performed just in the same way described in Kato et al. (2009) and Kato et al. (2012). The times of superhump maxima were determined using the template fitting method as described in Kato et al. (2009) after de-trending the global variation due to the outburst by using the locally-weighted polynomial regression (LOWESS; Cleveland 1979). The superhump periods were determined using phase dispersion minimization (PDM; Stellingwerf 1978) for period analysis and 1σ errors for the PDM analysis were estimated by the methods of Fernie (1989) and Kato et al. (2010).

¹ VSNET-alert archive can be accessed at <<http://ooruri.kusastro.kyoto-u.ac.jp/pipermail/vsnet-alert/>>.

² <<http://www.aavso.org/data-download>>.

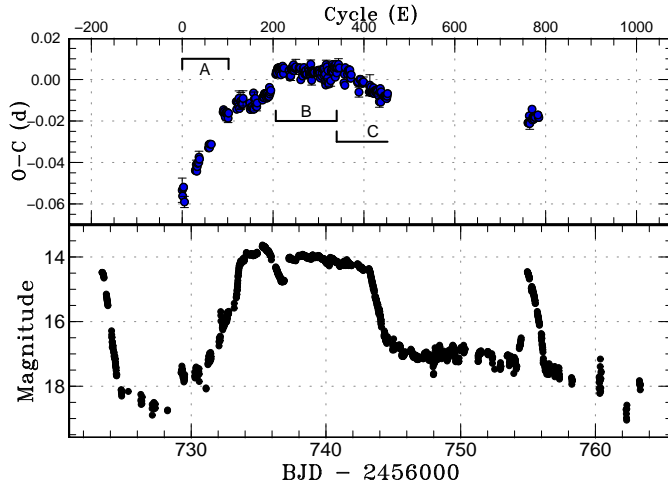


Fig. 1. $O - C$ diagram and light curve of J0902. (Upper) $O - C$ diagram. An ephemeris of $\text{Max}(\text{BJD}) = 2456729.3312 + 0.03372E$ was used to draw this figure. The intervals A–C represents superhump stages (see text for detail). The cycle counts between the main superoutburst and the rebrightening are uncertain. (Lower) Light curve. The observations were binned to 0.01 d.

4. Results

4.1. Outburst

Following the precursor outburst, the object remained in a state ~ 2 mag brighter than quiescence for 4 d (lower panel of figure 1). The object then started to brighten slowly, and the final rise to a superoutburst took place on BJD 2456733. After reaching the temporary maximum, the object again started fading (BJD 2456735–2456737). This fading episode (we call it a “dip”) was, however, temporary and the object then entered a plateau phase of the superoutburst for the next 6 d. The object then started fading from the superoutburst on BJD 2456743 at a rate of $\sim 1.8 \text{ mag d}^{-1}$. The object then remained around magnitude 17 (~ 3 mag brighter than quiescence) for 9 d. There was at least one post-superoutburst rebrightening on BJD 2456754–2456755. The fading from this rebrightening was also very rapid ($\sim 2.1 \text{ mag d}^{-1}$).

4.2. Superhumps

Superhumps started to appear during the slowly rising phase following the precursor (upper panel of figure 2). The superhumps observed in this interval had a long period, and this long period was observed for ~ 102 cycles (upper panel of figure 1). During the maximum before the temporary dip in the early part of the superoutburst, the period variation became more complex and the orbital period was detected as a transient signal. Following this temporary dip, the superhump period stabilized to a shorter period (lower panel of figure 2). There was a jump in the phase following the dip. The phase jump was significantly smaller than 0.5 phase, and this jump did not resemble a transition to the so-called “traditional” late superhumps (Vogt 1983). After a further ~ 140 cycles, the

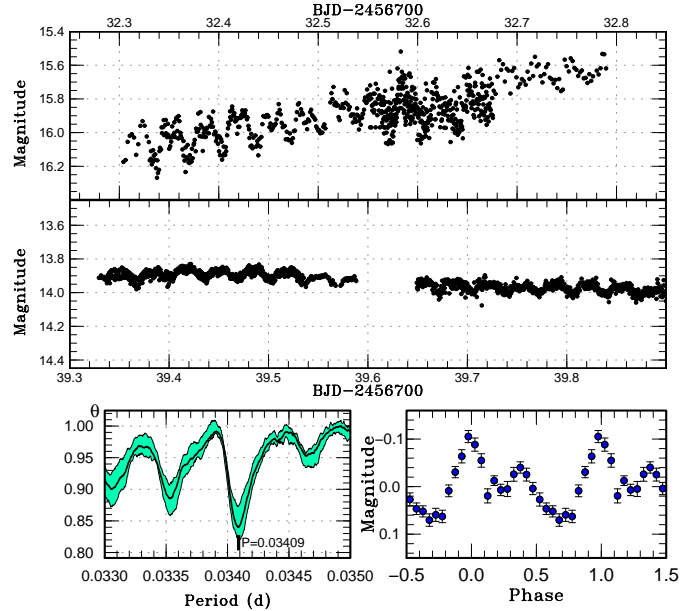


Fig. 2. Superhumps in J0902. (Upper) Superhumps in the rising stage of the superoutburst (stage A superhumps). (Middle) Superhumps after the “dip” phenomenon early in the main superoutburst (stage B superhumps). (Lower left) PDM analysis of stage A superhumps. (Lower right) Mean profile of stage A superhumps.

period again decreased discontinuously.

Based on the similarity of the $O - C$ diagram to those of recently identified candidate period bouncers in hydrogen-rich CVs (Kato et al. 2013; Nakata et al. 2014), we identified $E = 0 - 102$ (see upper panel of figure 1) as the growing stage of superhumps (stage A) and $206 \leq E \leq 340$ as stage B and $E \geq 340$ as stage C (for the superhump stages and the typical behavior in hydrogen-rich systems, see Kato et al. 2009). Although superhumps were continuously seen after the fading from the superoutburst plateau, the individual times of maxima are not shown on this figure due to the large errors in determination. There was a transition phase between stage A and B, which is unique to this object. The mean superhump periods in stages A, B and C were 0.03409(1) d, 0.03371(1) d and 0.03359(1) d, respectively.

5. Discussion

5.1. Outburst in a Long-Period AM Canum Venaticorum Star

Mass transfer in AM CVn-type objects is believed to be mainly powered by the gravitational wave radiation. Since the secondary is degenerate, the orbital period becomes longer as the secondary transfers the matter. As the systems evolve, the mass-transfer rates quickly decrease (Tsugawa, Osaki 1997; Nelemans et al. 2001a). It is known that helium accretion disks are prone to thermal instability, as well as in hydrogen-rich CVs, and systems with intermediate mass-transfer rates show dwarf nova

(DN) type outbursts (Tsugawa, Osaki 1997). This condition is usually considered to be achieved in systems with orbital periods of 20–40 min (Nelemans 2005). Long- P_{orb} objects like GP Com ($P_{\text{orb}}=46.57$ min) have never shown an outburst and are considered to have sufficiently low mass-transfer rates and possess stable cool disks. These expectations have generally been confirmed by observations (e.g. Ramsay et al. 2012).

J0902 has the longest P_{orb} among AM CVn-type objects which have ever shown outbursts [the previous record was CSS J045019.7–093113 having a superhump period of 47.28(1) min with some uncertainty in alias selection (Woudt et al. 2013)]. Nelemans (2005) suggested that the transition to the stable cool disks (without dwarf nova outbursts) happens between orbital periods of 34 and 39 min. The existence of two dwarf nova-type objects (J0902 and CSS J045019.7–093113) indicates that this transition happens in longer orbital periods (47–48 min). It would be an interesting question whether GP Com may undergo an outburst or whether GP Com has different properties despite the similarity of its orbital period with J0902.

5.2. Slow Evolution of Superhumps

In this object, it took more than 100 cycles to develop fully grown superhumps. AM CVn-type systems (at least for object with long orbital periods) are expected to have a very light secondary, and the small mass ratio is most likely responsible for the long duration of stage A since the growth rate of the superhumps is known to be proportional to q^2 (Lubow 1991; see a discussion in Kato et al. 2013). This finding is also compatible with the q estimation in the following subsection.

5.3. Estimation of the Mass Ratio from Stage A Superhumps

According to Kato, Osaki (2013), the precession frequency of stage A superhumps reflects the dynamical precession rate of the eccentric disk at the radius of the 3:1 resonance. The fractional superhump excess in frequency unit $\varepsilon^* \equiv 1 - P_{\text{orb}}/P_{\text{SH}}$ for stage A superhumps is 0.0158(18). This value corresponds to $q=0.041(7)$ (see table 1 or figure 2 in Kato, Osaki 2013). This result became the first measurement of the q value by this method in an AM CVn-type system. Since most of the error in q comes from the uncertainty in P_{orb} , this q value will be improved by further refinement of P_{orb} .

The q value of 0.041(2) for the eclipsing system SDSS J092620.42+034542.3 ($P_{\text{orb}}=28.31$ min) is comfortably close to the current estimate of J0902 (figure 3). The location of J0902 seems to be consistent with the theoretical evolutionary track representing the mass-radius relation for a semi-degenerate secondary [Tsugawa, Osaki (1997); see e.g. Yungelson (2008) for more detailed modeling].

The commonly used relation between fractional superhump excess and q [such as Patterson (1998), Patterson et al. (2005), Kato et al. (2009)] has uncertain errors due to the unknown pressure effect (cf. Kato, Osaki 2013), which is particularly the case for AM CVn-type objects (Pearson 2007). The value of $\varepsilon^*=0.0047(18)$ for stage B

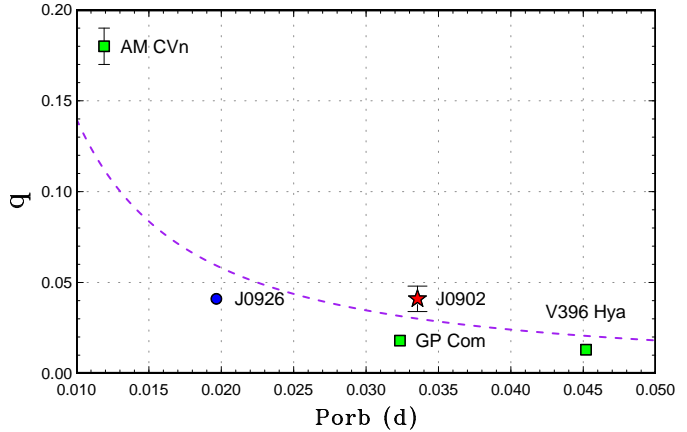


Fig. 3. Comparison of mass ratios in AM CVn-type objects. The filled circle represents the measurement from eclipse observations. The filled squares represent the measurements from Doppler tomography (AM CVn: Roelofs et al. 2006; GP Com: Marsh 1999; V396 Hya: Steeghs et al., in preparation, from Solheim 2010). The location of J0902 is shown with a filled star. The dashed curve represents equation (9) in Tsugawa, Osaki (1997) and assumed a $0.8 M_{\odot}$ primary.

superhumps in J0902 corresponds to $q=0.025(10)$ by the traditional method in Patterson et al. (2005); it is probable that the traditional method highly underestimate q values in AM CVn-type objects. We therefore did not include q values from superhumps (other than stage A) in figure 3. We propose that stage A superhumps provide an efficient and reliable tool for studying the evolutionary track of AM CVn-type objects.

5.4. Pressure Effect in Helium Disks

Pearson (2007) suggested that the pressure effect in helium disks may be higher than in hydrogen-rich disk since the ionization temperature is higher.

According to Lubow (1992), the apsidal precession frequency (ν_{pr}) can be written as a form:

$$\nu_{\text{pr}} = \nu_{\text{dyn}} + \nu_{\text{pressure}} + \nu_{\text{stress}}, \quad (1)$$

where the first term, ν_{dyn} , represents a contribution to disk precession due to the dynamical force of the secondary, giving rise to prograde precession; the second term, ν_{pressure} , the pressure effect giving rise to retrograde precession; and the last term, ν_{stress} , the minor wave-wave interaction. If we neglect the last term, we can estimate the contribution of the pressure effect by estimating $\nu_{\text{pressure}}/\nu_{\text{orb}}$, where ν_{orb} is the orbital frequency. In stage A, only ν_{dyn} contributes to the disk precession and in stage B, the combined effect of ν_{dyn} and ν_{pressure} is expected. We can thus estimate $\nu_{\text{pressure}}/\nu_{\text{orb}}$ by evaluating the difference between ε^* for stages A and B (see also Nakata et al. 2014).

In J0902, $\varepsilon^*(\text{stage A}) - \varepsilon^*(\text{stage B})$ is 0.012, which is not particularly larger than those in hydrogen-rich systems [0.010–0.015, figure 16 in Kato et al. (2009); see also Nakata et al. (2013)]. It will be worth pointing out that

the superhump period for stage B superhumps may be shorter than the orbital period if q is sufficiently small. This is expected to happen for $q \leq 0.03$ (Kato, Osaki 2013). If AM CVn-type dwarf novae with longer P_{orb} were to undergo superoutbursts, such a situation may be observed. The contribution of the pressure effect in helium disks needs to be examined further using more samples.

5.5. Transient Appearance of Orbital Signal

During the rising branch to the superoutburst maximum, a signal with a period very close to the orbital period was detected (vsnet-alert 17043). This signal was at the time considered to be early superhumps, which are supposed to arise from the 2:1 resonance in very low- q systems (cf. Osaki, Meyer 2002; Kato 2002). A similar period was also recorded during the late stage of the plateau phase and a competition between the 3:1 and 2:1 resonance was suggested (vsnet-alert 17082).

We re-examined this behavior. The variation of the superhump periods is shown in figure 4. The initial long period corresponds to stage A superhumps. There was a phase of transition between stage A and stage B, during which the period of superhumps showed a large variation. The initial appearance of the orbital signal corresponds to this phase (BJD 2456732). The second appearance was on a smooth continuation of stage B to C superhumps (around BJD 2456743). It is evident from this figure that the reported second appearance of the orbital signal was on the smooth extension of ordinary superhumps, and the period was slightly different from the orbital one. A combination of a very small q , shrinkage of the disk radius and the pressure effect apparently reduced the precession rate very close to zero. The situation for the initial appearance is less clear. Since the period was so close to the orbital period and the subsequent variation of the periods and the light curve were not regular, it may be indeed the case that the competition with the 2:1 resonance played some role in this phase. The profile of the superhumps in this phase, however, was not doubly humped as are commonly seen in early superhumps (Kato 2002).

The lack of long-lasting phase of early superhumps, which are commonly seen in WZ Sge-type dwarf novae (low- q , hydrogen-rich dwarf novae), can be understood considering that the main superoutburst apparently started as an inside-out-type (slowly rising) outburst, and the disk could not expand sufficiently to fully establish the 2:1 resonance. Such a phenomenon may be similar to those in candidate period bouncers, which are very low- q hydrogen-rich systems (Nakata et al. 2014).

This work was supported by the Grant-in-Aid ‘‘Initiative for High-Dimensional Data-Driven Science through Deepening of Sparse Modeling’’ from the Ministry of Education, Culture, Sports, Science and Technology (MEXT) of Japan. We acknowledge with thanks the variable star observations from the AAVSO International Database contributed by observers worldwide and used in this research. K. Antonyuk and N. Pit express a specific acknowledgement to the funding of the CCD Camera FLI

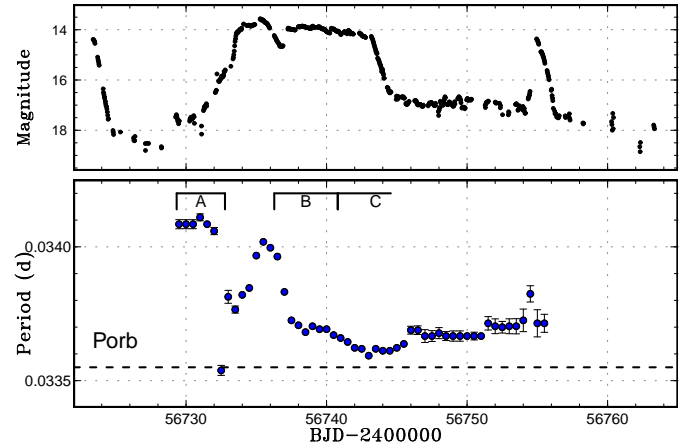


Fig. 4. Variation of the superhump period of J0902. (Upper) Light curve. The observations were binned to 0.03 d. (Lower) Superhump periods. The periods were determined from 3-d segments (shifted by 0.5 d) using the PDM method. The initial long period corresponds to stage A superhumps. There was a phase of transition between stage A and stage B, during which the period of superhumps showed a large variation. Superhump stages A–C are the same as in figure 1. The start of stage B and the distinction between stage B and C are not as clearly defined as in the $O-C$ diagram (figure 1) because the variation of the period is smeared by the use of 3-d segments.

ProLine PL230 by Labex OSUG@2020.

References

- Cleveland, W. S. 1979, *J. Amer. Statist. Assoc.*, 74, 829
Copperwheat, C. M., et al. 2011, *MNRAS*, 410, 1113
Ferne, J. D. 1989, *PASP*, 101, 225
Gorbvskoy, E. S., et al. 2013, *Astron. Rep.*, 57, 233
Hirose, M., & Osaki, Y. 1990, *PASJ*, 42, 135
Kato, T. 2002, *PASJ*, 54, L11
Kato, T., et al. 2009, *PASJ*, 61, S395
Kato, T., et al. 2012, *PASJ*, 64, 21
Kato, T., et al. 2010, *PASJ*, 62, 1525
Kato, T., Monard, B., Hamsch, F.-J., Kiyota, S., & Maehara, H. 2013, *PASJ*, 65, L11
Kato, T., & Osaki, Y. 2013, *PASJ*, 65, 115
Kato, T., Uemura, M., Ishioka, R., Nogami, D., Kunjaya, C., Baba, H., & Yamaoka, H. 2004, *PASJ*, 56, S1
Levitan, D., et al. 2014, *ApJ*, 785, 114
Lubow, S. H. 1991, *ApJ*, 381, 259
Lubow, S. H. 1992, *ApJ*, 401, 317
Marsh, T. R. 1999, *MNRAS*, 304, 443
Nakata, C., et al. 2014, *PASJ*, submitted
Nakata, C., et al. 2013, *PASJ*, 65, 117
Nelemans, G. 2003, *Classical and Quantum Gravity*, 20, 81
Nelemans, G. 2005, in *ASP Conf. Ser. 330, The Astrophysics of Cataclysmic Variables and Related Objects*, ed. J.-M. Hameury, & J.-P. Lasota (San Francisco: ASP), p. 27
Nelemans, G., Portegies Zwart, S. F., Verbunt, F., & Yungelson, L. R. 2001a, *A&A*, 368, 939
Nelemans, G., Steeghs, D., & Groot, P. J. 2001b, *MNRAS*, 326, 621
Osaki, Y., & Meyer, F. 2002, *A&A*, 383, 574

- Patterson, J. 1998, *PASP*, 110, 1132
- Patterson, J., et al. 2005, *PASP*, 117, 1204
- Pearson, K. J. 2007, *MNRAS*, 379, 183
- Ramsay, G., Barclay, T., Steeghs, D., Wheatley, P. J., Hakala, P., Kotko, I., & Rosen, S. 2012, *MNRAS*, 419, 2836
- Rau, A., Roelofs, G. H. A., Groot, P. J., Marsh, T. R., Nelemans, G., Steeghs, D., Salvato, M., & Kasliwal, M. M. 2010, *ApJ*, 708, 456
- Roelofs, G. H. A., Groot, P. J., Nelemans, G., Marsh, T. R., & Steeghs, D. 2006, *MNRAS*, 371, 1231
- Solheim, J.-E. 2010, *PASP*, 122, 1133
- Solheim, J.-E., & Yungelson, L. R. 2005, in *ASP Conf. Ser.* 334, 14th European Workshop on White Dwarfs, ed. D. Koester, & S. Moehler (San Francisco: ASP), p. 387
- Stellingwerf, R. F. 1978, *ApJ*, 224, 953
- Tsugawa, M., & Osaki, Y. 1997, *PASJ*, 49, 75
- Vogt, N. 1983, *A&A*, 118, 95
- Whitehurst, R. 1988, *MNRAS*, 232, 35
- Woudt, P. A., Warner, B., & Motsoaledi, M. 2013, *Astron. Telegram*, 4726
- Yungelson, L. R. 2008, *Astron. Lett.*, 34, 620